ANNALS OF THE UNIVERSITY OF CRAIOVA
ANNALES DE L'UNIVERSITÉ DE CRAIOVA

ANALELE UNIVERSITĂȚII DIN CRAIOVA

SERIA: INGINERIE ELECTRICĂ
SERIE: ELECTRICAL ENGINEERING
SÉRIE: INGÉNIERIE ÉLECTRIQUE
Anul/Year/Année 45
No. 45, Vol. 45, Issue 1, 2021

December 2021

ISSN 1842 - 4805

EDITURA UNIVERSITARIA

ANNALS OF THE UNIVERSITY OF CRAIOVA

13, A.I. Cuza Str., CRAIOVA 200585
ROMANIA

We exchange publications with similar institutions of country and from abroad

ANNALES DE L'UNIVERSITÉ DE CRAIOVA

Rue A.I. Cuza, No. 13, CRAIOVA 200585
ROUMANIE

On fait des échanges des publications avec les institutions similaires du pays et de l'étranger

This journal is published by the Faculty of Electrical Engineering from the University of Craiova.
The authors are fully responsible for the originality of their papers and for accuracy of their notes.

REVIEWERS COMMITTEE

Wireless Transfer of Electric Power - a Disruptive Technology

Andrei Marinescu
Romanian Academy of Technical Sciences, Craiova Branch Craiova, Romania
University of Craiova, Romania
ancor2005@gmail.com

DOI: 10.52846/AUCEE.2021.1.01

Abstract—**Wireless (contactless) transfer of electric power is a disruptive technology because it abandons wired transmission technology, the only technology used in electrical and electronic engineering until recently, just like in the past animal traction and film photography were replaced by mechanical traction and digital photography. Although revealed at the end of the nineteenth century through Tesla's inventions, it could be applied in practice only in the '80s of the twentieth century, with the development of power electronics and microprocessors. After an introduction and an overview of the operating principles, the paper presents the readiness level reached by this technology, the stage of standardization, Romanian achievements and future prospects for high power applications.**

Cuvinte cheie—*transmiterea puterii fără contact, tehnologie diruptivă, nivel tehnologic,expunere umană la câmp magnetic, aplicații*

Keywords—*wireless power transfer, disruptive technology, readiness level, magnetic field human exposure, applications*

I. Introduction

A disruptive technology, as defined by CM Christensen [1] is a technological innovation, a product or service, fundamentally different from the dominant technology on the market. One of the characteristics of disruptive technologies is that they coexist with existing technologies and are initially considered inferior by most consumers [2,3].

This category has included over time: the replacement of animal traction by mechanical traction and then by electrical traction, vacuum tubes replaced by transistors and then by integrated circuits, incandescent filament light bulbs replaced by the LEDs, HDDs by SSDs, 2D printers by 3D, 4D etc.

A similar paradigm shift in which the traditional transmission of electricity by conduction is replaced by the contactless transmission is a typical disruptive technology [4]. It is best known as Wireless Power Transfer (WPT) and has many important advantages in modern technology due to the absence of contacts and their wear, ease of use in aggressive or explosive environments, in air or water, with applications for both electric drives and for charging storage batteries in the most various fields such as: medicine, robotics, electric mobility, etc. The transfer of energy is carried out in the near field (magnetic or electric) on small and medium distances, with efficiency comparable to the transmission by galvanic contact and with the possibility of simultaneous transmission of power and data. Due to the different operating principle, both the theoretical bases and the simulation of circuits and fields through numerical methods are essential to the design and practical achievement of these systems in order to ensure interoperability, and increase the efficiency and the transferred power [5]. In [6] it is stated that: "*Wireless Power Transfer is now recognized as one of the 'Hottest' Research Areas in Electrical Engineering combining the EE Foundation Studies of Electricity and Magnetism with Power Electronics and Microprocessor Control*". This statement best summarizes the special endeavors in the field. The research into the IEEE Xplore database shows that in the field of inductive WPT alone during the period 2010-2020 [7] more than 1800 papers were published with an annual increase rate of 100%, plus over 6000 patents registered since Tesla patents until today, as evidenced by a search in the USPTO (U.S. Patent and Trademark Office) [8]. The papers on WPT listed above are featured not only in journals and conferences dedicated to power electronics applications but also in publications in related fields such as medicine, electromagnetic compatibility, etc. These figures are exceeded in number only by publications in the field of microelectronics. The IEEE Xplore database contains 32 papers in the field of Romanian authors, published after 2012 [7]. When the necessary high powers are transmitted, for example, to charge the batteries of an electric vehicle (EV) in static or dynamic charging systems, the limitation of human exposure to the stray magnetic field [9] requires electromagnetic shielding measures [10]. The autonomous driving systems of EVs on highways and in urban areas currently represent an important argument for the application of the contactless transfer of electric power. The paper analyzes the principles of designing inductive power couplers, the technological readiness level of these systems in contrast to plug-in charging, the evaluation and optimization of their parameters, the standards and regulations in force, the Romanian achievements for EVs and prospects for application in the near future.

II. Construction of Inductive Power Transfer Systems

A. *Realization and evaluation of power transfer through an inductive coupler*

The inductive coupler is an essential element of a WPT system. The simplest inductive coupler is shown in Fig. 1. It is in fact a two-port circuit with an input port and an output port usually consisting of two air core planar (circular or solenoidal) coils, loosely coupled, with self-inductances L_1 and L_2 and R_1 and R_2 with their AC value at operating frequency,. The primary coil is the transmitter (Tx) and the secondary coil is the receiver (Rx). Their position in the xyz coordinate system can be random, in the most general case; therefore the variable mutual inductance M largely determines the power transfer efficiency between the two ports. The gap between the coils (h) on z axis is the separation gap of the coupler which can be constant or variable depending on the application.

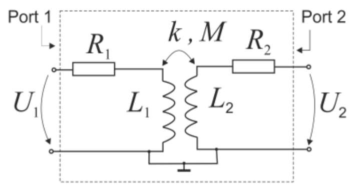

Fig. 1. Schematic diagram of the two-port inductive coupler.

M is calculated according to the known relation:

$$M = k(L_1\,L_2)^{1/2} \quad (1)$$

where *k* is the coupling factor of the two coils. In current practice, the value of k is small (0.1 – 0.2), which is why the circuit is considered loosely coupled.

The weak coupling is determined on the one hand by achieving a transfer distance as long as possible on z axis and on the other hand by the decrease of the power transfer sensitivity in the applications where the horizontal position of Tx against Rx (x, y axes) is variable (EV case) [6].

The value of $k(M)$ is usually increased by using magnetic flux concentrators made of ferrite material with different geometries [11].

For the calculation of the maximum power which can be transfered in the case of the inductive coupler in Fig.1, we start from the relation for the apparent power transmitted from port 1 to port 2:

$$S_2 = |U_{20}.I_{sc}| \quad (2)$$

where U_{20} is the voltage at the terminals of port 2 at no-load and I_{sc} is the short-circuit current generated at port 2.

After simple calculations using (1), we obtain:

$$S_2 = \omega.k^2.L_1.I_1^2 \quad (3)$$

or

$$S_2 = k^2.S_1 \quad (4)$$

where S_1 is the apparent power available in the primary Tx of the coupler.

Under these conditions, unlike the power transformer for which k~1, the Tx-Rx energy transfer indicated by S_2 is very low mainly due to the very high leakage inductances specific to the air core coils of the inductive coupler.

To increase the power transfer in WPT systems, the leakage inductances of the Tx and Rx coils are compensated by series or parallel capacitors.

Classical compensation topologies use simple LC-type networks, i.e. S-S, S-P, P-S and P-P (Fig. 2) in which the resonant frequencies of the primary and secondary are equal.

Under these conditions, regardless of the method of achieving the primary compensation, the relation (4) becomes:

$$S_2 = k^2.S_1.Q_2 \quad (5)$$

where Q_2 is the loaded quality factor of the circuit Rx at the operating frequency ω.

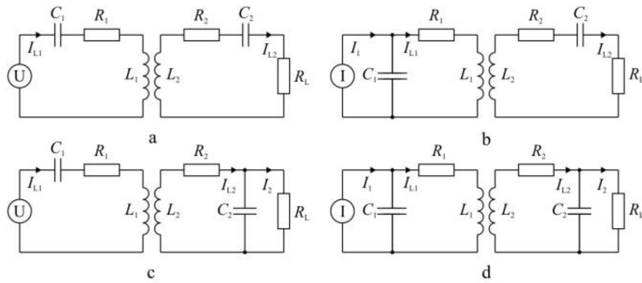

Fig. 2. The main inductive coupler compensation topologies. a-S-S, b-P-S, c-S-P, d-P-P.

Therefore the topologies in Fig.2 allow the practical realization of inductive WPT couplers with transfer outputs between 85 and 90 % when Tx and Rx are coaxial.

In order to be used in practice and compared in terms of efficiency, the S-S and S-P topologies are powered by voltage inverters and the P-S and P-P topologies are powered by current inverters as shown in Figs. 2.

There are a large number of parameters involved in the behavior of the inductive coupler, including: coil geometry, operating frequency, heat losses depending on the conductor used (solid or litz wire), winding step [12], magnetic field concentrators, loaded quality factor at operating frequency, etc.

Although they are simple and economical and therefore theoretically treated in many papers, the practical application of these topologies under variable load, short circuit, coupler coils offset, etc. affects both the operation of the primary inverter and the overall efficiency of the WPT system.

For these reasons, at high powers, when the stability and efficiency of the system is decisive, the application of hybrid compensation topologies with several energy accumulators has become widespread. The most common networks are the LCL and LCC topologies, symmetrical in the primary or secondary, or mixed (Fig. 3).

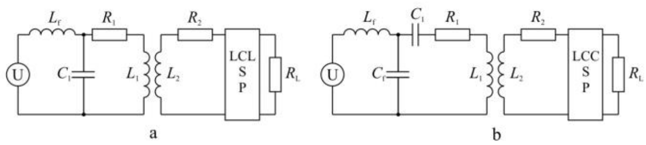

Fig. 3. Hybrid compensation topologies. a-LCL, b-LCC.

In the case of LCL topology [13] with a single resonant frequency, the series inductance L_f (usually equal to L_1) transforms the voltage inverter into a constant current inverter, the operation of which is load independent with a unit power factor.

In the case of LCC topology [14], the difference from LCL consists in inserting a capacity C_1 in series with L_1, which leads to the decrease of the inductive reactance of L_1 and, as a result, now $L_f < L_1$. The new circuit may have also a single resonant frequency given by $L_f.C_f = (L_1 - L_f).C_1$. Interoperability with other WPT systems is improved and the influence of the variation of the coupling factor produced by the coils offset (misalignment) as well as the Tx - Rx air gap is smaller.

To make a comparison of the performance of inductive couplers, their factor of merit (FOM) [15], a dimensionless parameter determining the transfer efficiency is defined and can be determined based on the relation:

$$\mathrm{FOM} = kQ = \omega M/R \quad (6)$$

where Q and R represent the geometric averages of the quality factors, respectively of the AC resistances of the two coils.

The transfer efficiency can be expressed as:

$$\eta_{max} \approx 1 - 2/kQ \quad (7)$$

The maximization of product kQ is a necessary measure, but the reduction of k (unjustifiably increased gap between the coupler coils) must be carefully controlled in practical applications because it greatly influences the operating mode of the inverter used.

The process of evaluation of a prototype coupler begins by analyzing the constructive variants achieved by simulation with 2D or 3D finite element; the physical optimized model is achieved and finally the values of the characteristic parameters (L, R, M, k, Q) obtained by simulation are compared with those experimentally determined; the experimental method described in [16] using a vector network analyzer (VNA) with impedance meter function is useful (Fig.4).

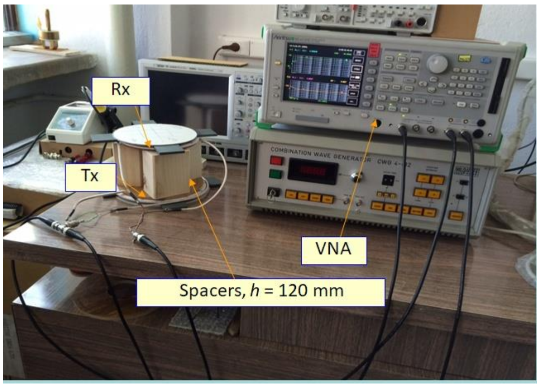

Fig. 4. Lab evaluation of the parameters of an inductive coupler with VNA.

Currently, inductive couplers are designed for transferred powers of 3.7 - 22 kW for EVs or 100 - 300 kW for electric buses and even 1MW for Maglev trains and ferries [17].

At transfer powers of over 50 kW, the inductive coupler has either a structure consisting of three coils powered by single or three-phase inverters [18], or has a modular construction consisting of four or six coplanar coils powered by single-phase inverters with synchronized operation [19].

Fig. 5 shows the laboratory test of the complete prototype of a inductive WPT system consisting of: frequency converter, Tx - Rx resonant circuits, microcontrollers, rectifier, filter and artificial load resistor which in this case replaces the charging battery.

The main qualification tests which must be performed on a WPT system are at least the following: efficiency test, PFC and power test, air gap and offset flexibility, magnetic field emissions according to the standards in the following paragraph.

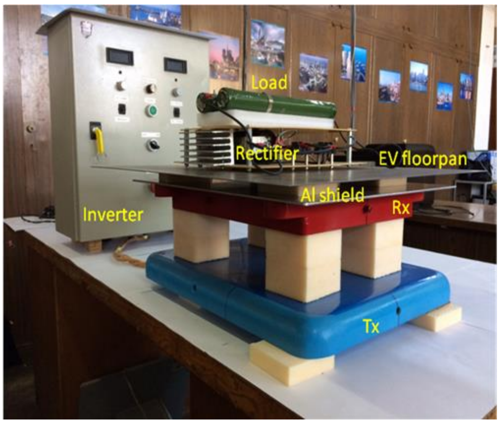

Fig. 5. Testing an EV WPT system for 3.7 kW in the laboratory. At the upper part (above Rx) there is the Al shield (2 mm thick) over which a steel plate (3 mm thick) simulates the EV chassis.

B. Standardization of WPT systems

The standards cited below are the result of extensive international collaboration. The IEC standards marked as CD (Committee Draft) are versions in the stage of final approval. The American standard, SAE J2954 [20] is the first WPT standard published as final version in 2020.

Although the standards are not mandatory, they are still fundamental elements of conduct for designers but also for researchers when approaching a new concept and especially when this concept, although original, must be compatible with other existing systems.

As proof, the success of Qi wireless mobile charging system developed by Witricity [21], currently produced on a large scale by companies worldwide is based on the publication of the company standards by IEC [22].

The main standards related to the WPT are:

- IEC 61980-1:2020, Electric Vehicle Wireless Power Transfer (WPT) Systems – Part 1: General requirements;

- IEC 61980-2, Ed. 1, (CD), Electric Vehicle Wireless Power Transfer (WPT) Systems – Part 2: Specific requirements for communication between electric road Vehicle (EV) and infrastructure with respect to wireless power transfer (WPT) systems;

- IEC 61980-3, Ed. 1, (CD), Electric Vehicle Wireless Power Transfer (WPT) Systems – Part 3: Specific requirements for the magnetic field wireless power transfer systems;

- ISO 19363:2020 Electrically propelled road vehicles – Magnetic field wireless power transfer - Safety and interoperability requirements;

- SAE J2954:2020 Surface Vehicle Standard – Wireless Power Transfer for Light-Duty Plug-in Electric Vehicles and Alignment Methodology.

The SAE standard J2954 [20] has adopted the LCC topology [14] and considers the whole set of problems that ensure the industrialization of WPT transfer systems, i.e. interoperability, frequency band, electromagnetic compatibility, protection of living beings from the magnetic stray field and last but not least the optimization of the design of the inductive coupler, which is the result of tests performed on actual systems in the laboratory and in operation for powers between 3.7 and 11 kW.

C. Operating frequency of wireless power transfer systems

The general rule governing any WPT system, whether it is intended for data or power transfer is its non-conflicting co-existence with radio communication systems, which is why the ITU (International Telecommunication Union) established the so-called ISM frequency band for industrial, scientific and medical equipment [23], which includes fixed frequencies from 6.78, 13.56, 27 MHz to 2.4 GHz and above. Some of these frequencies are used for magnetic resonance-based power transfer systems [24].

Furthermore in [23], by an international agreement, the use a non - ISM frequency band in the range 10 - 100 kHz is allowed for WPTs charging, namely:

1. 42 – 48 kHz and 52 – 58 kHz for light EVs;
2. 19–21 kHz and 59 – 61 kHz for heavy electric vehicles (buses) with charging powers of 75 - 300 kW;
3. 85 ± 0.5% kHz proposed by SAE J2954 [20] for light EVs with charging powers of 3.7 – 11 kW using low voltage AC grid.

The main reason that led to this choice is related to the fact that WPT systems have interference emissions in very confined areas around the equipment/vehicle because in the near field the magnetic component decreases proportionally by $1/d^3$ and, as a result, they are considered localized sources of magnetic field or Short Range Devices (SRDs) [25].

The frequency range 1 (42–48 kHz) was used for the prototype built so far in Romania [26], solely due to the available litz wire (elementary wire with a diameter of 0.2 mm). Currently there are litz wires with an elementary wire of 0.05 - 0.071 mm which can be used to approach operating frequencies up to 200 kHz The transition to range 3 (85 kHz) is in progress for the second generation WPT of the same EV.

D. Block diagram of a WPT system

Fig. 6 shows this block diagram vs. the similar diagram used for plug-in charging [27]. The most important difference is the replacement of the isolation transformer with an inductive coupler and its compensation circuits that form a critical area with a significant share in the overall efficiency in the absence of a careful planning of its parameters.

Both systems must contain active filters on the supply side so as not to generate harmonics in the supply network, taking into consideration the high powers flowing through them. It can be noted that, in the case of WPT systems, the onboard part includes fewer components. As a result, the energy transfer efficiency of the two systems can be comparable under a suitable design.

When using modern semiconductor components with SiC [28], the current overall efficiency of the WPT exceeds 90 % when the offset of the coupler coils is within the limits allowed by the system.

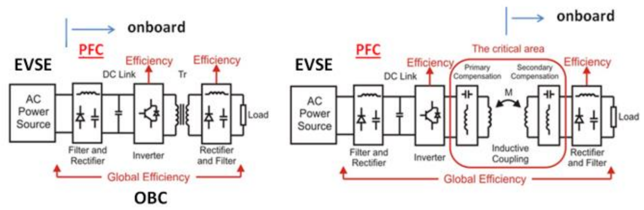

a b

Fig. 6. Comparison between the block diagrams of plug-in equipment (a) and WPT (b). EVSE-Electric Vehicle Service Equipment, OBC-OnBoard Charger, PFC-Power Factor Correction.

E. Storage batteries as a load for the inverter used for the WPT system

In most cases, the WPT systems are used to charge storage batteries, the charging mode of which is a combination of constant current (CC) charging followed by a final constant voltage (CV) charging as shown in Fig. 7.

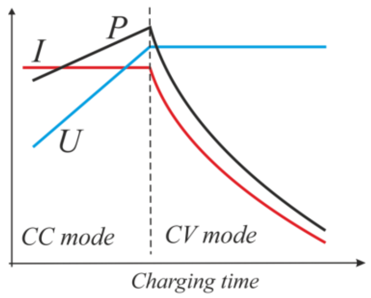

Fig. 7. Typical quantities in the storage battery charging process.

During this process, the inverter operates at variable power (P) in both CC and CV mode, noting that its peak power is generated at the end of the constant current area, and then it decreases 5 - 7 times in the constant voltage area.

This operating mode must be taken into account when designing the system by using current and voltage sensors in the automatic control loop so that the efficiency of the inverter is not affected. In the case of EVs, the charging/discharging mode is governed by the specific “C” parameter which represents the battery charging/discharging rate (C-Rate). It represents the numerical value of the ratio (A/Ah) of the charging/discharging current in A to the battery capacity in Ah. A normal charge is to 0.15 C which means, for example, for a 60 Ah battery, a 10A charging current for about 6 hours. Traction Li-Ion batteries are sized for 1 or 2 C mode. Fast or ultra-fast charging of certain EV batteries can be performed to 3 C (180 A in 20 minutes in the above case) or even to 4 C, under continuous temperature monitoring and forced cooling, a process performed on this systems [29]. Improving the control algorithms of the state of charging (SOC) and state of health (SOH) of the battery is one of the current endeavors of the research in the field so that the concerned regime will neither affect the operating safety, nor the battery life [30].

In the case of WPT charging, it should be noted that this is a typical intermittent charging system: the battery is charged automatically, without operator intervention, every time the EV reaches a public charging station and parks there even for a few minutes. This operating mode results in lower power consumption and increased battery life. In the case of urban electric buses, the system is widely practiced on the route or at the end of the line where it is called “opportunity charging”.

III. Technological Readiness Level of WPT Systems

There are technical influencers who consider that the technologies based on the wireless transmission of information and more recently of power are inefficient and dangerous to health although all studies conducted so far do not lead to this conclusion [31].

In the case of the WPT there is still an opinion that the power and transfer efficiency are low as opposed to plug-in transmission. The actual situation is as follows: on the one hand WPT equipment with powers up to 300 kW was built and used in practice on buses [19] and, on the other hand, for the plug-in charging system, losses were not considered: in the transformer from the charging station, in the connection cables, in the connectors, in the charger on board the EV which provides the AC/DC conversion. The overall efficiency of any equipment is the product of the partial efficiencies of the blocks in the system. If equal efficiencies of 97% are considered in theory in the case of four blocks, an overall efficiency of 89% will be reached! For a current WPT system, the efficiency is comparable to the plug-in system, i.e. 85 - 90% [32].

In both cases, the transition from Si semiconductors used in current power electronics to SiC or GaN semiconductors will increase the overall efficiency by at least 95%.

Since it is a disruptive technology, the number of WPT pieces of equipment in operation so far is relatively small, because the “technological readiness level” or TRL is lower. Regardless of the field of activity, TRL [33] defines 1 - 9 stages of maturity and TRL 4-6 is considered the bridge between scientific research and engineering application.

In the case of WPT, the highest level (9) has been reached (meaning “Technology proven through successful operations”) by some companies: KAIST (Korea), Conductix – Wampfler (Germany), Plugless Power (US) etc mentioned in the FP 7 ”FABRIC” project [34], but there are many other companies with level 7 – 8 achievements.

In Romania, the activity in the WPT field started almost 10 years ago in several university centers and research institutes is mostly focused on theoretical and experimental research included in doctoral theses, bachelor’s theses and scientific publications and less on functional models or prototypes which have reached in some cases the TLR level 3, i.e. “demonstrating the functionality of the concept, in relation to the critical functionalities of the system, through analytical and experimental studies”. The explanation for this situation consists, to a certain extent, in the almost non-existent funding offered by the Romanian Research Authority for this disruptive technology.

In Romania the highest known level is level 6 [35] in which the real-scale prototype, capable of fulfilling all the functions required by the operating system was tested in an environment relevant to the real operating conditions.

IV. WPT Charging System for Dacia Electron Ev and Other Applications

The DACIA Electron automobile based on the mechanical structure of the Dacia Sandero automobile was built by CCIA (R&D Center for the Automobile Industry) at the University of Pitesti with the support of Renault RTR Romania in 2016 and publicly presented in 2017 at the EV Show 2017 [27]. It has a “combined charging system” consisting of the classic plug-in system and a WPT Charging system built by ACER Romania [36] in collaboration with INDA-Eltrac SRL, Craiova [37] (Fig. 8).

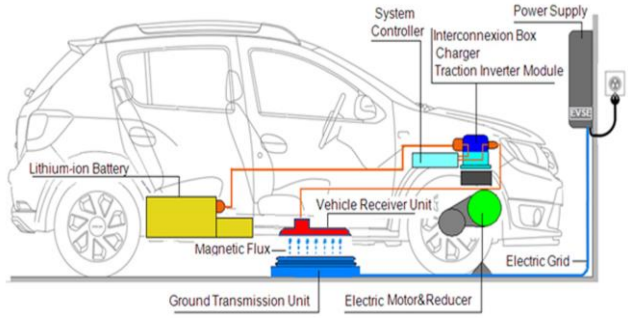

Fig. 8. WPT charging system mounted on DACIA Electron EV [27].

This is an industrial prototype (TRL 6) with a standardized load power of 3.7 kW for a ground clearance ranging between 80 and 110 mm (currently increased to 140 mm). It performs the CC-CV charging cycle for a modern cobalt-free LPF (LiFePO4) battery [35] of 12.3 kWh, with the voltage of 205 V and weight of 160 kg. The range of this EV is at least 100 km.

The prototype is our starting point for R&D on WPT power transfer systems with powers over 1 kW, such as:

- urban rail vehicles (catenary-free trams);
- buses, minibuses, vans and commercial vehicles;
- unmanned aerial vehicles (UAV);
- unmanned underwater vehicles (UUV);
- factory transportation equipment including autonomous (AGV);
- robotics and radar rotating platforms

Assessment of Human Exposure to the Magnetic Field Generated by the WPT

Although basically there is no person inside the EV during battery charging, the limits set by ICNIRP [9] for the protection of persons who are for various reasons in the vicinity or passing by must be observed and certified by measurements performed by accredited laboratories. Fig. 9 presents a comparison of the evolution of the permissible level of exposure during 1998 – 2010 [9].

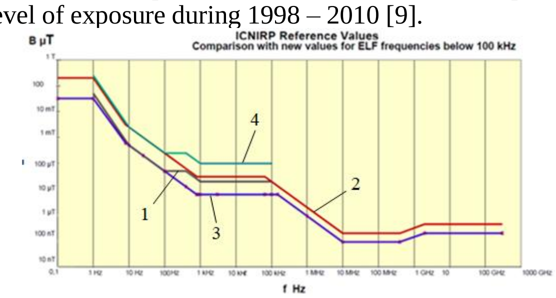

Fig. 9. Evolution of the ICNIRP [9] exposure level during 1998 - 2010: 1-occupational 1998, 2-public 2010, 3-public 1998, 4-occupational 2010.

In the 10 - 100 kHz frequency range of interest for inductive WPT systems, a relaxation took place: the level of magnetic field allowed for the public has increased from 6.25 μT to 27 μT and for workers from 50 μT to 100 μT. This increase is the result of applying the precautionary principle on which international standards for exposure to electromagnetic radiation are generally based.

The distance at which the measurement is taken is 500 mm from the edge of the inductive coupler or 300 mm from the side edge of the EV at a height of 0.7 m from the ground. An example of 42 kHz operating frequency measurements for DACIA Electron is shown in Fig. 10 a, b, highlighting the asymmetrical position of the Rx receiver required by the design of this vehicle chassis (Sandero) to maintain the ground clearance. The level of 27 μT is exceeded only in that area (34 μT) To decrease the *B* value below 34 μT (red) to 22 μT, additional shielding of Rx was required.

a)

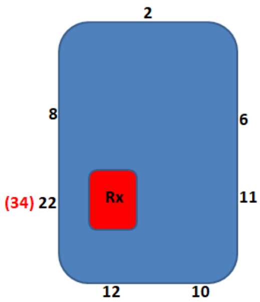

b)

Fig.10. Magnetic B field in μT around EV DACIA Electron. a) Rx location, b) Three-dimensional measured B values for 3.7 kW transferred power (top view).

V. WPT Perspectives and Associated Problems

At present it is clear that, regardless of the current opinion of users of automobiles with internal combustion engines, EVs are already winning due to the measures to limit the manufacture and use of Diesel engines in some EU countries. In the very near future EVs will become autonomous and connected vehicles and then it will not be possible to design an autonomous EV without an automatic battery charging based on WPT.

Discussions that the use of EVs aggravates pollution caused by fossil fuels used to increase the electricity generation in conventional power plants are unjustified for two reasons: first, environmental pollution is especially dangerous in large urban areas and then, the renewable sources associated with energy storage systems will totally or partially compensate for the increase in electricity consumption [38]. In addition, as the number of EVs increases, they will be able to provide, if necessary, the electricity needed in certain critical situations by using bidirectional inverters (conversion of G2V to V2G system).

It should be noted that the change of the current paradigm in urban electric mobility is also under discussion, by building small EVs (less than 2 m in length), with a range limited to 30-50 km, parked perpendicular to the road and charged right there by WPT according to the expression: “Smaller, lighter, greener”. Such examples already exist in the mass production [39], while EVs with the current dimensions to be intended for long-distance travel.

Here are some of the concerns of the near future related to electric mobility and wireless power transfer:

- Accelerated generalization of electric public transport in urban areas (buses, commercial vehicles, etc.);

- Increasing the public acceptability of the WPT [40];

- The improvement of the WPT energy transfer efficiency up to 95%, by using modern switching circuits with SiC or GaN;

- The transition from the plug-in system to the WPT system with a transitory coexistence period;

- The recycling used Li-Ion batteries taking into account the limited global reserves of Li, Co, etc.;

- The achievement of virtual power plants (static storage from renewable energy sources) and the expansion of individual prosumer systems [38];

- Realization of fast and ultra-fast EV charging stations and coordination of energy consumption through Smart Grid technique;

- Generation of EVs artificial noise to warn cyclists and pedestrians (the probability of an accident caused by EVs is twice as high as opposed to vehicles fitted with internal combustion engines) [41];

- Promoting Romanian WPT R & D projects within the national cluster network “WPT Rom Net” [42] open to all research institutions and production companies, local public administration authorities, employers’ associations or professional associations, legal entities and individuals interested in contributing to the development and practical application of WPT knowledge.

- Publishing in English, to increase the visibility of Romanian research in the field, using also the special dedicated issues of the “Annals of the University of Craiova - Electrical Engineering Series” [43].

VI. Conclusions

The paper aims to draw the attention of potential users and funders to the applications and benefits of wireless power transfer (WPT).

The WPT has many advantages for the most diverse applications of modern technology due to the absence of contacts and their wear, ease of use in aggressive or explosive environments, conductive liquids (marine environment), the possibility of simultaneous power transfer and data communication and its efficiency comparable to plug-in systems on short and medium distances, at power levels reaching tens or hundreds of kW.

The paper provides a brief overview of the technical solutions, applications and perspectives offered by the WPT in light of the growing interest in reducing pollution in large cities and the prospect of large-scale use of autonomous and connected EVs.

A practical example is the 3.7 kW industrial WPT prototype built for charging the battery fitted on EV DACIA Electron.

The integration in the Smart Grid of EVs fast/ultra-fast charging stations, including renewable energy sources, energy storage systems and proper management of energy sources and energy demand will result in energy efficient solutions.

ACKNOWLEDGMENT

The paper is part of the scientific activities of the National Network WPT Rom Net [42].

Received on July 20,2021
Editorial Approval on November2, 2021

REFERENCES

[1] CM Christensen, *The Innovator's Dilemma, when new technologies cause great firms to fail*, Harvard Business School Press, Boston, Ch 10, pp159-171, ISBN 0-87584-585-1, 1997.

[2] Innovation Society, https://innovatingsociety.com/

[3] Susan Adams, Clayton Christensen, *On What He Got Wrong About Disruptive Innovation*, Available: https://www.forbes.com/sites/forbestreptalks/2016/10/03/clayton-christensen-on-what-he-got-wrong-about-disruptive-innovation /? sh = 76472bd4391b .[Accessed: 15-May-2021]

[4] The Disruptive Potential of Wireless EV Charging, Available: https://www.navigantresearch.com/reports/the-disruptive-potential-of-wireless-ev-charging . [Accessed: 13-Apr-2021]

[5] A. Marinescu, Georgiana. Rosu, L. Mandache, O. Baltag, "Achievements and Perspectives in Contactless Power Transmission", *EPE 2018 Conference*, Iasi, October 2018.

[6] JT Boys, GA Covic, "The Inductive Power Transfer Story at the University of Auckland", *IEEE Circuits & Systems Magazine*, Vol.15, Issue 2, May 2015, pp: 6-27.

[7] Search for Inductive WPT Electric Vehicles Publications in IEEE Xplore Archive, Available on: https://ieeexplore.ieee.org/search/searchresult.jsp?queryText=inductive%20power%20transfer% 20for% 20Electric% 20Vehicles & highlight = true & returnFacets = ALL & returnType = SEARCH & matchPubs = true & ranges = 2010 2020 Year , [Accessed: 07.20.2021].

[8] USPTO-US *Patent and Trademark Office*, Available on: https://www.uspto.gov/ , [Accesed: 07.20.2021]

[9] ICNIRP Guidelines for Limiting Exposure to Time - varying Electric and Magnetic Fields (1 Hz - 100 kHz), Health Physics 99 (6), pp. 818-836, 2010.

[10] K. Jiseong, K. Jonghoon, K. Sunkyu, K. Hongseok, S. In-Soo, S. Nam Pyo, et al., "Coil Design and Shielding Methods for a Magnetic Resonant Wireless Power Transfer System", *Proc. IEEE*, vol. 101, No. 6, pp. 1332-1342, 2013.

[11] TH Kim, S. Yoon, JG Yook, GH Yun, WY Lee, "Evaluation of power transfer efficiency with ferrite sheets in WPT system," *2017 IEEE Wireless Power Transfer Conference (WPTC)*, 2017, pp. 1 -4, two: 10.1109 / WPT.2017.7953894.

[12] A. Marinescu, I. Dumbravă, "AC Resistance of Inductive Coupler with Pitch Coils for Contactless Power Transfer", *International Conference on Applied and Theoretical Electricity (ICATE)* , October 4 - 6, 2018, Craiova, Romania.

[13] L. Tan,, S. Pan, C. Xu, C. Yan, H. Liu, X. Huang, "Study of Constant Current-Constant Voltage Output Wireless Charging System Based on Compound Topologies", *Journal of Power Electronics*, Vol. 17, No. 4, pp. 1109-1116, July 2017.

[14] J. Deng *et al*., "Frequency and Parameter Combined Tuning Method of LCC-LCC Compensated Resonant Converter with Wide Coupling Variation for EV Wireless Charger", in *IEEE Journal of Emerging and Selected Topics in Power Electronics*, two: 10.1109 / JESTPE.2021.3077459.

[15] T. Ohira, "The kQ Product as Viewed by an Analog Circuit Engineer", *IEEE Circuits and Systems Magazine*, First Quarter 2017, pp.27-32.

[16] A. Marinescu , I. Dumbravă , "Using VNA for IPT Coupling Factor Measurement", *2016 IEEE International Power Electronics and Motion Control Conference* (PEMC) .

[17] G. Guidi, JA Suul, F. Jenset and I. Sorfonn, "Wireless Charging for Ships: High-Power Inductive Charging for Battery Electric and Plug-In Hybrid Vessels", in *IEEE Electrification Magazine*, vol. 5, no. 3, pp. 22-32, Sept. 2017, two: 10.1109 / MELE.2017.2718829.

[18] K. Kusaka, R. Kusui, J. Itoh, D. Sato, S. Obayashi, and M. Ishida, "A 22 kW-85 kHz Three-phase Wireless Power Transfer System with 12 coils", *IEEE Energy Conversion Congress and Exposition (ECCE*), Baltimore, MD, USA, 2019, pp. 3340-3347.

[19] A. Calabro, B. Cohen, A. Daga, J. Miller and F. McMahon, "Performance of 200-kW Inductive Charging System for Range Extension of Electric Transit Buses", *2019 IEEE Transportation Electrification Conference and Expo (ITEC*), 2019, pp. 1-5, doi: 10.1109 / ITEC.2019.8790490.

[20] SAE J2954: - SAE J2954: *2020 Surface Vehicle Standard-Wireless PowerTransfer for Light-Duty Plug-in / Electric Vehicles and Alignment Methodology*

[21] Witricity, Qi Interface, Available on: http://www.wirelesspowerconsortium.com/ [Accesed: 6.10.2021] Available: http://www.wirelesspowerconsortium.com/

[22] IEC PAS 63095-1.2: 2017, "Interface definitions" and "Reference Designs".

[23] ITU-R Report SM.2303-2, 2017, *Wireless Power Transmission using Technologies other than Radio Frequency Beam*, pp.29-33.

[24] M.Kesler, *Highly Resonant Wireless Power Transfer: Safe, Efficient, and over Distance*, Witricity White paper, 2017.

[25] M. Feliziani and S. Cruciani, "Mitigation of the magnetic field generated by a wireless power transfer (WPT) system without reducing the WPT efficiency", *Proc. INT Symp. Electromagn. Compat. (EMC - EUROPE)*, 2013, pp. 610-615.

[26] DG Marinescu, V. Nicolae, F. Serban, I. Vieru, N. Mierloiu, N. Boicea, A. Marinescu, A.Vintila, „An Electric Crossover Concept Car", *EVS30 Symposium* Stuttgart, Germany, October 9 - 11, 2017.

[27] A.Marinescu, I.Dumbrava, A.Vintilă, DG Marinescu, D.Neagu, V.Nicolae, A.Radu, „The Way to Engineering EV Wireless Charging: DACIA Electron", *EV 2017* (Electric Vehicles International Conference & Show), Bucharest, 2017.

[28] B. Basille, J. Rangaraju, „Wich new semiconductor technologies will speed electric vehicle charging adoption", *AN SLIY005*, pp 1-7, Texas Instruments Inc, 2017.

[29] C. Suarez, W. Martinez, "Fast and Ultra-Fast Charging for Battery Electric Vehicles - A Review," *2019 IEEE Energy Conversion Congress and Exposition (ECCE)*, 2019, pp. 569-575, doi: 10.1109 / ECCE.2019.8912594.

[30] S. Zhang, H. Sun, C. Lyu, "A method of SOC estimation for power Li-ion batteries based on equivalent circuit model and extended Kalman filter", *2018 13th IEEE Conference on Industrial Electronics and Applications (ICIEA*), 2018, pp. 2683-2687, doi: 10.1109 / ICIEA.2018.8398164.

[31] R. Bosshard, JW Kolar, "Inductive power transfer for electric vehicle charging: Technical challenges and tradeoffs", *IEEE Power Electronics Magazine*, vol. 3, no. 3, pp. 22-30, Sept. 2016.

[32] Gereon Meyer (Ed), *Advanced Microsystems for Automotive Applications*, Springer, 2012, Ch.5, pp. 49-52

[33] Horizon 2020, Work Program 2016-2017, General Annexes, pp. 35-44, Available on: https://ec.europa.eu/programmes/ horizon2020 / en / what-work-program , [Accesed on 5.20.2021]

[34] M. Emre, P. Vermaat, D. Naberezhnykh, Y. Damousuis, T. Theodoropoulos, V. Cirimele, A. Doni, "D 3.3.1 - Review of existing power transfer solutions", *Public Deliverable EU FABRIC project (605405)*, 2014.

[35] A. Marinescu, A. Vintila, DG Marinescu, V. Nicolae, "Development of a wireless battery charger for Dacia Electron EV," *10th*

International Symposium on Advanced Topics in Electrical Engineering (ATEE), pp. 241-247, 2017

[36] ACER (Romanian EMC Association), Available on: www.acero.ro/ , Accessed: 14.07.2021

[37] INDAELTRAC SRL, Available on: https://www.indaeltrac.com/ , Accessed: 20.07.2021

[38] N. Golovanov, A. Marinescu, „Power Supply of EV Charging Stations in a Smart Grid (in Romanian)”, *The 13th edition of the Conference "ASTR Days"* October 17-19, 2018, Ploiești, Romania.

[39] WJ Mitchell, Ch. E. Borroni-Bird, LD Burns, *Reinventing the Automobile-Personal Urban Mobility for the 21st Century*, 227 pp. , The MIT Press, Cambridge, Massachusetts, 2010

[40] Sylvia Heyvaert, O. Hegazy, Th. Coosemans, J. Van Mierlo, „Social Acceptance of Wireless Battery Charging Systems: Belgium Case Study”, *2014 IEEE International Electric Vehicle Conference* (IEVC), 2014, pp. 1-6, doi: 10.1109 / IEVC.2014.7056075 .

[41] *Silent Revolution: Engine Sound Design for EVs*, Available on: https://interestingengineering.com/silent-revolution-engine-sound-design-for-evs , Accessed: 20.06.2021

[42] A. Marinescu, „The Romanian Wireless Power Transfer Network”, *JESI Journal of Engineering Sciences and Innovation*, Electrical and 149-156, 2020

[43] "Wireless Power Transfer" Special issue of *Annals of the University of Craiova*, Vol. 42, Issue 1, pp. 47, 2018

Application of the Rotor Field-Oriented Control for an Induction Motor Used in Electric Traction

Mihaela Popescu*, Alexandru Bitoleanu* and Constantin Vlad Suru*
* University of Craiova, Faculty of Electrical Engineering, Craiova, Romania, mpopescu@em.ucv.ro

DOI: 10.52846/AUCEE.2021.1.02

***Abstract* – In this paper, the rotor field-oriented control is applied for a three-phase induction motor used in electric traction of an autonomous locomotive powered by a battery. First, the operating equations in the rotor field-oriented system are introduced. Then, the control scheme based on the structural scheme and operational equations are presented. After referring to the design of the controllers, the performances of the control system during the start-up process by prescribing a ramp speed and step rotor flux are addressed and analyzed. Four values of the prescribed speed are taken into consideration. Through the presented results, the synthesis of the control system and control algorithm are validated.**

Cuvinte cheie: *control cu orientare după fluxul rotoric, tracțiune electrică, locomotivă autonomă, motor trifazat de inducție, regulator cu histerezis, regulator PI.*

Keywords: *rotor field-oriented control, electric traction, autonomous locomotive, three-phase induction motor, hysteresis controller, PI controller.*

I. Introduction

In the 1970s, Haase [1] and Blaschke [2] introduced the so-called field-orientation technique applied to the induction motor, which involves decoupling the torque and magnetic flux as with the direct current motor. In a reference frame that rotates simultaneously with the rotor flux, the torque can be controlled by the q-axis component of the stator current vector.

The best known implementation of the rotor field-oriented control is the indirect control. According to this, the rotor flux is estimated and not measured, based on the associated equations [3].

When the voltage control is taken into consideration, two control paths exist in the structure of the rotor field-oriented control [4]-[6]. Within the first path, the external loop is of the speed and the subordinate loop is of the active current. In the second path, the external loop is of the rotor flux and the subordinate loop is of the reactive current.

The difficulty in the implementation of the voltage control consists of the need to design four controllers. But, if a control structure with current control is adopted, only two controllers remain in the system to be designed and the inverter control is performed by a hysteresis controller [6].

Among the challenges of implementing the rotor field-oriented control, the accurate estimation of the motor parameters and ensuring the most precise control of the current's components are highlighted [7]-[14]. In [11], the proposed strategy involves the use of the rotor field-oriented model equations to estimate the electromagnetic torque and rotor resistance.

To estimate the rotor resistance, the authors of [10] designed a scheme based on the rotor flux model and fuzzy controller. In [14], a sensorless fuzzy logic based indirect vector control with an adaptation scheme for the rotor resistance using neural learning algorithm was taken into consideration.

An adaptive sliding-mode observer was proposed in [8], and the online adaptation of the rotor resistance was achieved. A sliding mode observer based on rotor-flux was presented in [12] and a predictive field-oriented controller was used.

To keep the speed and torque of the induction motor oriented on the rotor field during the supply voltage drop, a new control technique was analyzed in [13], in which the d-axis and q-axis current control is based on solving the voltage, current, and torque constraints in the current plane.

The results presented in this paper were obtained by carrying out the PACETSINEFEN project in the frame of POC program, European Regional Development Fund. The implementation of the proposed control system will be done on an electric traction physical model of a locomotive powered by a battery.

The next part of this paper is organized as follows. In section II, the operating equations and control scheme are presented. Next, the attention is directed to the synthesis of speed and rotor flux controllers. Then, section IV presents the performance of the system, in which, the start-up process by prescribing a ramp speed and a step rotor flux, for four prescribed speeds, are taken into consideration. The paper ends with some conclusions and future research directions.

II. Operating Equations and Control Scheme

The equation of operation are expressed in the (d, q) reference frame with the d-axis oriented in the direction of the rotor flux (Fig. 1). As shown, the q-axis component of the rotor flux is zero. λ is the angle between the rotating (d, q) reference frame and the fixed reference frame (α, β).

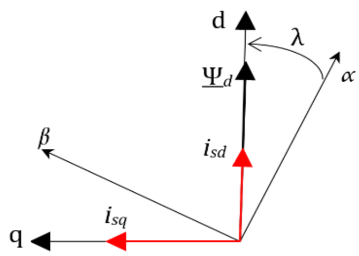

Fig. 1. Orientation of the rotating (d, q) reference frame.

The following expression of the electromagnetic torque shows that, if the rotor flux is constant, the electromagnetic torque can be controlled only through the q-axis component of the rotor current.

$$m = -\frac{3}{2} p \Psi_{rd} i_{rq}. \tag{1}$$

The equations of the rotor circuit are [15]:

$$0 = R_r i_{rd} + \frac{d}{dt}\Psi_{rd}; \tag{2}$$

$$0 = R_r i_{rq} + (\omega_1 - p\omega)\Psi_{rd}, \tag{3}$$

where the expressions of the rotor flux on the two axes are:

$$\Psi_{rd} = L_r \mathrm{i}_{rd} + L_m \mathrm{i}_{sd}; \tag{4}$$

$$0 = L_r \mathrm{i}_{rq} + L_m \mathrm{i}_{sq}. \tag{5}$$

The equation of motion is added to the system of equations.

$$J\frac{d\omega}{dt} = -\frac{3}{2} p \Psi_{rd} \mathrm{i}_{rq} - m_s. \tag{6}$$

The following quantities are used in equations (1) - (6):

$\underline{i}_r$, $\underline{\Psi}_r$ - the spatial phasors of the rotor currents and rotor flux referred to the system (d, q);
m, m_s – the electromagnetic and static torque respectively;
R_s, R_r – the stator and rotor resistances referred to the stator;
L_r – the inductance on a rotor phase referred to the stator;
L_m – the magnetization inductance;
p – the number of pole pairs;
ω – the angular velocity of the rotor;
ω_1 – the electrical speed of the rotating coordinate system.

The adopted control structure shown in Fig. 2 involves the current control, which is easier to implement compared to the voltage control. As shown, to synthesize the control signals for transistors, a three-phase hysteresis controller (Hys) is used. The existence of two controllers (Rω for speed and Rψ for the rotor flux), the transformation blocks for the reference frame ((d,q) →(α,β) and (α,β)→(a,b,c)) and the speed transducer (Tω) is highlighted. The rotor flux is calculated based on the stator current and the motor speed and the position angle λ of the rotating reference frame is calculated based on the sine and cosine functions, as follows [6], [15]:

$$\cos\lambda = \frac{\Psi_{s\alpha}}{|\Psi_r|}; \quad \sin\lambda = \frac{\Psi_{s\beta}}{|\Psi_r|}. \tag{7}$$

As illustrated in Fig. 2, there are two independent control paths, for speed and active current control and for rotor flux and reactive current respectively.

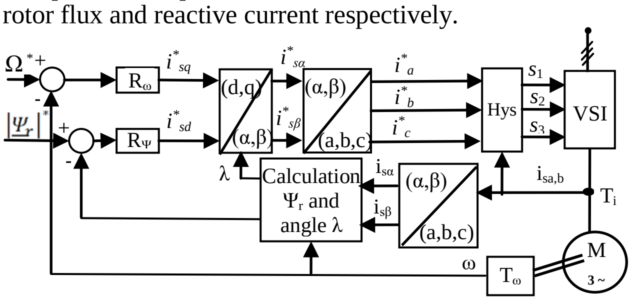

Fig. 2. Structure of the control system with current control.

In the first path, the prescribed active current is obtained at the output of the speed controller, whereas, in the second path, the prescribed reactive current is obtained at the output of the flux controller.

III. Synthesis of Speed and Rotor Flux Controllers

To express the involved transfer functions of the two controllers, the operational equations in the Laplace domain were used [6].

The parameters of the PI speed controller ($\theta_{1\Omega}$ and θ_{Ω}) which intervene in its transfer function,

$$G_{R\omega}(s) = \frac{1 + s\theta_{1\Omega}}{s\theta_{\Omega}}, \tag{8}$$

were determined using the symmetry criterion [6].

$$\theta_{1\Omega} = 4T_{\Sigma}; \quad \theta_{\Omega} = \frac{8K_f T_{\Sigma}^2}{T_m}, \tag{9}$$

where T_{Σ} is the dead time of the active current control loop (the sum of the speed transducer time constant and the sampling time T_s), the amplification factor K_f is:

$$K_f = \frac{3pL_m\,\psi_{rN}}{2L_r}\frac{\Omega_N}{T_N}, \tag{10}$$

and the mechanical time constant (T_m) is:

$$T_m = \frac{2JL_r\Omega_N}{3pL_m I_N\,\Psi_{rN}}. \tag{11}$$

The parameters of the PI flux controller ($\theta_{1\psi}$ and θ_{ψ}) in the transfer function,

$$G_{R\Psi}(s) = \frac{1 + s\theta_{1\Psi}}{s\theta_{\Psi}}, \tag{12}$$

were provided by using the Modulus criterion in Kesller variant [6].

IV. Control System Performance

The performance of the control system was assessed by using a specific Matlab-Simulink model developed for the experimental test platform. Table I summarizes the main parameters of the voltage source inverter and traction motor and Table II contains the parameters of the two controllers.

TABLE I.
MAIN PARAMETERS OF THE VOLTAGE SOURCE INVERTER AND TRACTION MOTOR

Inverter parameters								
U_{in} (V)	U_{Nout} (V)	P_N (kVA)	f_N (Hz)	f (Hz)	C_d (μF)	U_{CdN} (V)	IGBTs	
750	500	190	50	0-135	1400	1800	CM2400HC-34H	
Traction motor rated parameters								
U_N (V)	P_{2N} (kW)	f_{1N} [(Hz)	I_N (A)	$\cos\varphi_N$	η_N	s_N	n_N (rpm)	M_N (Nm)
500	155	45	218	0.888	0.924	0.02518	1316	1125
R_1 (Ω)	X_{1N} (Ω)	$L_{\sigma1}$ (mH)	R_2 (Ω)	X_{2N} (Ω)	$L_{\sigma2}$ (mH)	R_m (Ω)	X_m (Ω)	L_m (mH)
0.035	0.0621	0.2197	0.0358	0.067	0.2387	89.38	3.2507	11.497

TABLE II.
PARAMETERS OF THE SPEED AND FLUX CONTROLLERS

$K_{p\Omega}$	$T_{i\Omega}$	$K_{p\Omega}$	$T_{i\Omega}$	$K_{p\psi}$	$T_{i\psi}$
$\Omega_p \geq \Omega_N/2$		$\Omega_p < \Omega_N/2$		36	0.32
100	0.003	200	0.004		